INTERNATIONAL SOCIETY FOR SOIL MECHANICS AND GEOTECHNICAL ENGINEERING



This paper was downloaded from the Online Library of the International Society for Soil Mechanics and Geotechnical Engineering (ISSMGE). The library is available here:

https://www.issmge.org/publications/online-library

This is an open-access database that archives thousands of papers published under the Auspices of the ISSMGE and maintained by the Innovation and Development Committee of ISSMGE.

The paper was published in the proceedings of the 7th International Conference on Earthquake Geotechnical Engineering and was edited by Francesco Silvestri, Nicola Moraci and Susanna Antonielli. The conference was held in Rome, Italy, 17 - 20 June 2019.

A numerical study of ultimate lateral capacity of pile groups

B. Becci & N. Cardella CEAS s.r.l., Milano, Italy

M. Carni

Harpaceas s.r.l., Milano, Italy

ABSTRACT: In current design practice, analysis of pile groups subjected to lateral loads is mainly focused on the assessment of overall stiffness and on force distribution within the group. In contrast, the estimate of ultimate lateral capacity is often considered in a quite rough manner or even neglected. Such practice may be due by the fact that, traditionally, lateral loads onto pile groups were a quite low percentage of vertical loads; moreover, technical difficulties in carrying out full scale tests represented a serious obstacle in collecting experimental data to be used in the definition of reliable lateral methods for the estimate of lateral capacity of groups. More recently, however, reliable numerical tools may partially surrogate or integrate experimental data to assist engineers in defining design methods. In the light of such approach, a numerical study of laterally loaded groups of large diameter piles with fixed head conditions is presented. By means of commercial code FLAC3D, several models are studied, including most of the aspects affecting actual behavior, such as nonlinear soil response, pile-soil interface as well as plastic resistance of piles. Based on several analyses results, a very simple design method is proposed, which can be seen as an extension of classic Broms method. By means of this approach, which can be easily programmed in a spreadsheet, several aspects that affect laterally capacity of pile groups can be easily highlighted and some practical recommendations can also be obtained.

1 INTRODUCTION

Pile groups are one of the most common solutions for the foundation of many civil engineering structures such as tall buildings, bridge piers and abutments, high tanks or silos and so on. In current practice as well as in most popular design standards such as Eurocodes, an abundant amount of recommendations is available to address their design. However, looking more deeply into available material, some aspects that need further developments remain. One of such topics is represented by the design of pile groups subjected to relevant lateral forces. While several design approaches are available and widely used to assess pile groups behavior under lateral loadings which are quite lower than ultimate group capacity, in contrast a limited number of methods is available to reliably assess ultimate capacity. Such deficiency has become even more apparent with the increasing importance of lateral loads onto pile groups, in particular due to seismic design.

A review of existing literature on this topic reveals that available theoretical or experimental studies on ultimate lateral capacity of pile groups are quite limited mainly due to the intrinsic complexities of this problem which is governed by a tight interaction between geotechnical and structural aspects. Such difficulties also rest in the practical complexities in setting up full scale loads tests which are usually just conducted on single piles.

As for practical designs, group efficiency is often used. Such factor is normally defined as

$$\eta = \frac{Group \, reaction}{n_p \cdot (reaction \, of \, one \, pile \, acting \, as \, single)} \tag{1}$$

in which n_p is the number of piles in the group and the reaction is a pile (or group) force corresponding with a given top deflection.

Such parameter can be of course defined with respect to vertical or lateral response. In the first case, η is currently defined with respect to a quite low deformation level, thus giving a measure of group efficiency with respect to group stiffness. In contrast, such approach is rarely adopted in defining vertical capacity. As for lateral behavior, a different η factor is usually defined, to scale the so-called p-y curves that still very frequently adopted in modelling the interaction of piles with surrounding soil: in this respect, again, η should be considered as a matter of stiffness rather than of resistance. However, in such case the same (or very similar) η factor used to scale p-y curves is frequently also used to calculate group ultimate lateral capacity, based on the ultimate capacity of single piles. Such procedure, in our opinion, may be often inappropriate since group behavior at failure may differ significantly from the behavior of single piles. Moreover, by simply taking an efficiency factor into account without looking more in details in group behavior, unsafe design of crucial structural details may result. In the light of these simple observations stemming from current practice, a simple proposal is worked out in following, which may contribute to improve current design of laterally loaded pile groups.

2 A SIMPLE MODEL FOR LATERAL GROUP CAPACITY ASSESSMENT

Ultimate lateral capacity H_{ult} of single piles or pile groups intimately depends on both surrounding soil resistance and on structural bending capacity of pile cross sections. As for single pile capacity, such behavior at failure has been excellently explained by Broms, whose proposals (Broms (1964a, 1964b), still stand as a fundamental contribution widely used in the practice. As it will be shown in the following, Broms theory also produces results in a very close agreement with numerical models.

An attempt to extend Broms approach to a piling group with a regular geometrical pattern is presented in the following. We limit our attention to closely spaced pile group in a homogeneous granular soil, whose resistance is expressed by a friction angle φ . Following Fleming et al. (2009), or Patra & Pise (2001), we consider a block failure mechanism in which soil resistance is fully activated on the front side (passive resistance) (Figure 1) and along lateral sides.

Driving active thrust at rear face is neglected, since it represents a small fraction of other components. As for n_B piles in the front row, passive soil resistance from pile top to depth x, acting on a front width B, is given by

$$R_{front}(x) = K_P \cdot B \cdot \left(q \cdot x + \frac{\bar{\gamma} \cdot x^2}{2} \right)$$
 (2)

in which K_P is passive thrust coefficient depending on ϕ , q is uniform surcharge at soil surface (included as recommended by Cecconi et al. (2006)) and is soil unit weight, which must be set equal to buoyancy weight for water table at pile top. B is given by

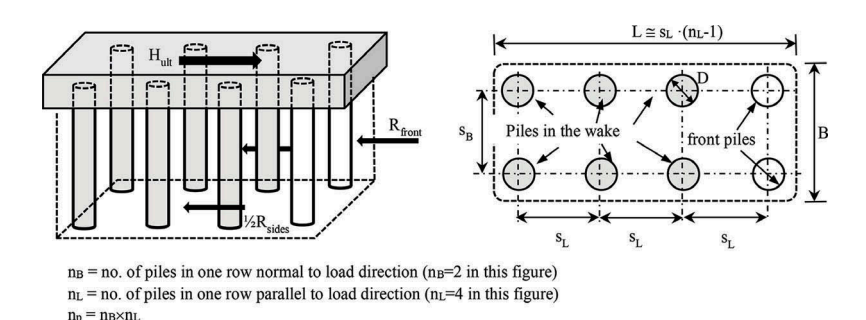


Figure 1. Pile group geometry and symbol definition

$$B = \min(3 \cdot D \cdot n_B, D + (n_B - 1) \cdot s_B)$$
(3)

In Equation 3, it is assumed that for quite distant piles, B is simply the sum of passive resistance pertaining single piles, which is set equal to $3 \cdot D$ according to Broms formulation. We now limit our analysis to long piles fully restrained at pile top, which represents the most common assumption occurring in the practice. Ultimate resistance for such piles is reached when two plastic hinge form, one at pile top and one at an unknown depth x_1 . By observing that at such depth, the shear forces in yielding piles is null, corresponding with a maximum M_y in bending moment distribution, we can compute x_1 by simply imposing moment equilibrium for piles above that depth:

$$2 \cdot n_B \cdot M_y - K_P \cdot B \cdot \left(q \cdot \frac{x_1^2}{2} + \frac{\bar{\gamma} \cdot x_1^3}{3} \right) = 0 \tag{4}$$

This equation is easily solved by an iterative procedure and then the contribution of front piles to overall resistance is obtained by substituting x_1 in Equation 2. It should be noted that setting q=0, $n_B=1$ and setting K_P to Rankine value, classical Broms (1994a) formulation is reproduced. We now consider all the piles behind the front ones, in other words $n_B \cdot (n_L-1)$ piles in the wake of the leading ones. We will assume that all of them equally contribute to the resistance provided by soil resistance at the sides. This contribution is assumed to be:

$$R_{\text{sides}}(x) = 2 \cdot K_{\text{LAT}} \cdot \tan(\phi) \cdot L \cdot \left(q \cdot x + \frac{\overline{\gamma} \cdot x^2}{2} \right)$$
 (5)

L is defined in Figure 1. K_{LAT} is a lateral earth pressure coefficient, for which Fleming et al. (2009) recommend considering a value ranging between at rest coefficient K_0 and 1. As a matter of fact we found that K_{LAT} plays an important role in the calculation of H_{ult} , so much more attention to it will be given in following section. Like front piles, we will assume that all the piles in the wake, equally loaded by same fraction of R_{sides} , will form a plastic hinge at pile top and a second one at the same depth x_2 . As before, we compute x_2 by solving

$$2 \cdot n_B(n_L-1) \cdot M_y - K_{LAT} \cdot tan(\phi) \cdot L \cdot \left(q \cdot \frac{x_2^2}{2} + \frac{\bar{\gamma} \cdot x_2^3}{3}\right) = 0 \tag{6} \label{eq:6}$$

Finally, overall pile group capacity is

$$H_{ult} = R_{front}(x_1) + R_{sides}(x_2) \tag{7}$$

It is worth noting that, by including the same bending capacity M_y for all the piles, different values for x_1 and x_2 are obtained, being usually $x_2 > x_1$. This means that lower plastic hinges form at different depth, depending on pile position in the group. Assigning same moment capacity is really a very crude assumption since bending capacity is affected by axial forces in piles. However, this assumption greatly simplifies the formulation and we also believe that including a safely assessed average value in the light of applied loads may provide a reasonable estimate of ultimate capacity as well. Implementing equations 1 to 7 in a spreadsheet, a very quick estimate of group capacity for various group patterns can be obtained. A most valuable result is also group efficiency η with respect to ultimate conditions, by dividing H_{ult} by the number of piles and by the single pile capacity (Broms value). For example, taking ϕ =33°, K_P = 3.39, q=0, =18 kN/m³, D=1 m, M_y =1500 kN·m, s/D = 3, in both direction, we obtain ultimate capacities and group efficiencies summarized in Table 1 for various pile patterns.

Beyond ultimate capacity values, a relevant result provided by this procedure is an increased depth of lower plastic hinge in shadowed piles, as compared with front piles. This observation suggests to carefully increase pile reinforcement fairly below the depth that would have been requested by single pile solution. R_{sides} , x_2 and η are significantly affected by K_{LAT} . In this respect, an attempt to better assess such parameter deserves additional attention.

Table 1. some results using Equations 1 to 7

Case	$n_{\rm B}$	$n_{ m L}$	K_{LAT}	R_{front}	\mathbf{x}_1	R_{sides}	\mathbf{x}_2	H_{ult}	η
				[kN]	[m]	[kN]	[m]	[kN]	
0	1	1	n.a.	1229	3.66	n.a.	_	1229	n.a.
1	2	2	0.7	2457	3.66	1384	6.50	3841	0.781
2	2	2	1.0	2457	3.66	1559	5.77	4016	0.817
3	2	4	0.7	2457	3.66	3907	6.91	6365	0.648
4	4	2	0.7	4915	3.66	2197	8.19	7122	0.724
5	2	4	1.0	2457	3.66	4401	6.16	6858	0.698
6	4	2	1.0	4915	3.66	2427	7.27	7389	0.752

3 A NUMERICAL STUDY

3.1 Approach description

To attempt a rational selection of governing parameters of the proposed procedure, in particular K_{LAT} factor governing block side resistance, a set of benchmark results would be necessary. However, in our best knowledge, it is quite hard to access enough experimental data covering relevant conditions for practical applications. Therefore, we considered performing some advanced numerical simulations of typical groups using the commercial code FLAC3D (Itasca (2018)). Such models include following main components:

- a uniform soil layer to which Mohr-Coulomb constitutive model is assigned;
- piles (o single pile) which are modelled as elastic perfectly plastic pipes, in such a way to model reinforced concrete shafts with a known bending capacity;
- a slip interface between pile and soil, whose resistance is assigned through a friction angle δ.

At the top of the piles, fixed head support condition is modelled by prescribing same lateral movement \bar{u} to all the grid points of a portion of piles projecting above soil surface (Figure 2). For each pile pattern, including single pile conditions, a FLAC 3D analysis has been performed, according with following sequence:

- a. set up of initial at rest condition by assigning an initial K₀ stress field
- b. insertion of piles (and their interface)
- c. progressive increase of top displacement \bar{u} , with 20 increments of 1 cm each, up to a final displacement of 20 cm.

Such procedure is accomplished by means of the nonlinear explicit pseudo-dynamic integration scheme offered by FLAC3D, by simply applying prescribed velocities for a suitable number of steps. Between each displacement increment, additional cycles with null velocities are performed, until overall top reaction (i.e. the resultant of all the lateral reactions where lateral displacement is assigned) is stabilized. In this study, only 1000 mm dia., 20 m long concrete piles are considered, in a granular dry soil. Pile spacing s/D =3 is kept constant in all the analyses, as such value corresponds with the most frequent spacing adopted in the practice. Additional parameters are: soil modulus E=100 MPa, ν =0.30, dilatancy ψ =0°, $\bar{\gamma}$ =18 kN/m³, K₀=0.5, E_{pile}=25 GPa.

Several models have been analyzed, by varying pile pattern (including single pile models to allow a comparison with Broms predictions), ϕ , δ and M_y . For all such models a top load-displacement curve is computed. In Figure 3, typical FLAC3D model is shown: one half of the group is modelled due to geometry and load symmetry. The model is extended, far from loaded zone, about 20 m in front and behind external piles in load direction as well as far from outer piles in lateral direction. A 10 m thick soil layer is considered under pile toe. Horizontal displacements normal to each boundary plane are fixed. In Table 2, a summary of performed analysis is included, corresponding with a total amount of 40 analyses.

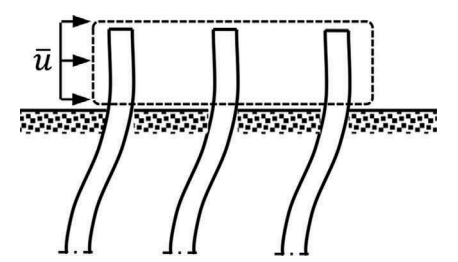


Figure 2. prescribed boundary condition at pile top

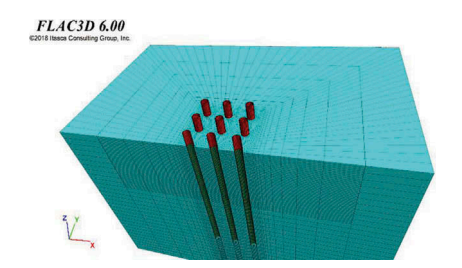


Figure 3. Typical FLAC 3D model: in this case a model with $n_B = 5$ and $n_L = 3$ is shown.

Table 2. summary of parameter variations

	pattern		ф	δ/φ	M _y
	$n_{\mathbf{B}}$	$n_{\rm L}$			[kN·m]
single	1	1	30°	0.5	1050
2×2	2	2	36°	1	2100
3×3	3	3			
3×5	3	5			
5 × 3	5	3			

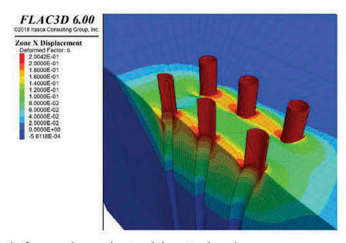
3.2 Result summary

In Figure 4, some typical results are shown. In Figure 4(a) a contour map of displacement highlights a block failure mechanism encompassing all the piles, combined with a more complex deformation field between single pile rows parallel to load direction.

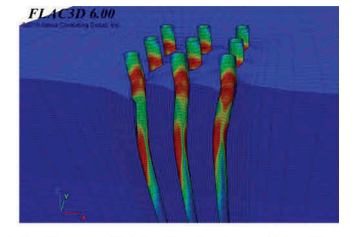
In Figure 4(b) we can appreciate different plastic zone development in piles, depending on pile position. As anticipated in previous section, lower plastic zone (plastic hinge) is deeper for piles in the wake of the front ones. In Figure 5, nonlinear overall behavior is shown at early deformation stages, while ultimate load is almost reached at a top displacement of about 10%D. Such behavior is the same for all the investigated cases. Moreover, it is noticed that group efficiency increases with top displacement. Such results may be explained by the fact that at low deformation, elastic interaction between piles prevails, thus reducing overall stiffness; when limit state is almost reached, yielding in soil somehow reduces the coupling between adjacent piles thus reducing group reduction with respect to the sum of single pile responses. Such finding, however, is in contrast with other studies (e.g. Fayyazi et al. (2014), Rollins et al. (2005)) and suggests further research to be clarified. However, an important conclusion from this study is that group efficiency is strictly related to the level of mobilization at which is computed

An overview of the performed analyses is included in Table 3, left part.

In the <u>right part</u> of Table 3, for each analysis, group capacity is computed by means of the proposed approach in section 2. To obtain a close agreement with FLAC3D results, two



(a) deformed mesh at ultimate load



(b) plastic zone distribution (red zones) in piles

Figure 4. typical FLAC 3D results.

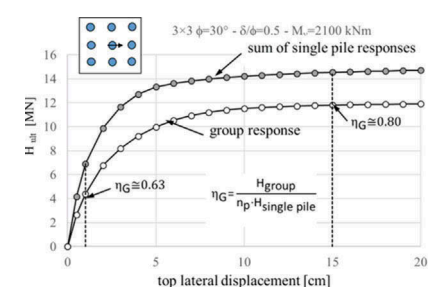


Figure 5. group response computed by FLAC3D.

important aspects had to be included, namely 1) a K_P value depending also on δ/ϕ , by adopting the passive thrust coefficients suggested by Lancellotta (2006) and 2) a quite high K_{LAT} value set equal to K_P as well, a value much higher than those recommended by previously cited authors, but, as theoretically expected, closely related just to soil resistance. By comparing the deformed shapes and plastic zones in piles in FLAC3D with computed plastic hinge depth with simplified approach, a quite satisfactory agreement is also observed. Efficiency coefficients computed by current study both by FLAC3D and by simplified approach, are in general higher than those frequently adopted in the practice (for example, Callisto & Rampello (2013), Fayyazi

Table 3. FLAC3D Analysis summary and comparison with proposed formulation

			FLAC3D			Proposed formulation with $K_{LAT}=K_P$ $\phi=30^{\circ}$				
			φ=30°							
		$\delta/\phi \rightarrow$	0.5		1		0.5		1	
pattern		$My \rightarrow$	1050	2100	1050	2100	1050	2100	1050	2100
single 2 × 2	H _{ult} ^(*) H _{ult}		1004 3641	1634 5808	1093 4042	1808 6327	1047 4014	1662 6372	1104 4233	1753 6719
3 × 3	$\eta_G \ H_{ m ult} \ \eta_G$		0.91 7476 0.83	0.89 11908 0.81	0.92 8184 0.83	0.87 13092 0.80	0.96 7954 0.84	0.96 12626 0.84	0.96 8387 0.84	0.96 13313 0.84
3 × 5	$H_{ult} \ \eta_G$		11592 0.77	18206 0.74	12668 0.77	19917 0.73	12531 0.80	19892 0.80	13213 0.80	20974 0.80
5 × 3	$ m H_{ult}$ $ m \eta_G$		12342 0.82 φ=36°	19840 0.81	13518 0.82	21758 0.80	12000 0.76 φ=36°	19050 0.76	12645 0.76	20086 0.76
		$\delta/\phi \to$	0.5		1		0.5		1	
pattern	ļ	$My \rightarrow$	1050	2100	1050	2100	1050	2100	1050	2100
single 2 × 2	$egin{aligned} H_{ult} \ H_{ult} \ \eta_G \end{aligned}$		1153 4227 0.92	1937 6739 0.87	1202 4673 0.97	2101 7490 0.89	1190 4735 0.99	1889 7516 0.99	1281 5097 0.99	2033 8091 0.99
3 × 3	H_{ult} η_G		8641 0.83	13854 0.79	9619 0.89	15273 0.81	9472 0.88	15036 0.88	10198 0.88	16188 0.88
3 × 5	H_{ult} η_{G}		13413 0.78	21178 0.73	14910 0.83	23299 0.74	15087 0.85	23949 0.85	16242 0.85	25782 0.85
5 × 3	H_{ult} η_{G}		14298 0.83	22908 0.79	15936 0.88	25372 0.80	14247 0.80	22616 0.80	15338 0.80	24347 0.80
	(*) H _{ult}	in [kN]								

et al. (2014), Viggiani et al. (2012)). As already discussed, such relevant discrepancy rests in the fact that previous values have been estimated corresponding with low deformations and/or different top restraint conditions. This observation, however, suggests that using traditional group factors tuned for group stiffness, also for group capacity is a conservative assumption.

4 A PROPOSAL FOR PRACTICAL DESIGN

In Figure 6, left, predicted capacities obtained by proposed equations are compared with FLAC3D analysis results. Aiming at providing a safe formulation in which all result points fall below the dotted line, proposed equation results have been multiplied by reduction factor 0.90: doing so all the results point are brought into safe region (Figure 6, right). In general, the agreement is better for almost square patterns ($n_B=n_L$). For unsymmetrical case 5×3, simplified approach seems to be very conservative: this may be explained in the light of a more complex actual failure mechanism dissipating more plastic work than what is assumed by simple block scheme. In such case, a more complex scheme, as proposed by Ashour et al. (2004) may provide better agreement.

By inspecting FLAC3D results, a simple equation for efficiency factor can also be obtained, which has the ability to account for both overall number of piles in a group and their configuration with respect to applied loads. We define a group efficiency with respect to ultimate capacity, which can be computed by the following equation:

$$\eta_{G,ult} = 0.9 \cdot (n_B)^{-0.025} \cdot (n_L)^{-0.15}$$
 (8)

Ultimate capacity of single pile can be computed by either Broms formulation or equivalent equations in section 2, including improved K_P coefficients accounting for appropriate δ/ϕ parameter. Group capacity is computed by using efficiency as per Equation 8 which already includes a reduction factor 0.90. Finally, the depth of reinforcement cage to be provided to ensure the validity of the assumed formulation can be assessed by the following iterative procedure:

- a. calculate $\eta_{G,ult}$ using Eqn. 8;
- b. iteratively calculate group capacity using equations 1 to 7, by progressively reducing K_{LAT} (starting with K_{LAT} = K_P) until same $\eta_{G,ult}$ is obtained.
- c. record lowest hinge depth corresponding with the last reduced K_{LAT} factor;
- d. provide adequate pile reinforcement down to such depth plus at least 3 pile diameters, to all piles in the group.

Of course, an appropriate design of piles subjected to lateral forces is not only affected by calculation approach, but also by a good selection of construction detailing. What is required to ensure overall lateral capacity must be compared with ordinary pile analysis via p-y curves and the most stringent values must be adopted in design.

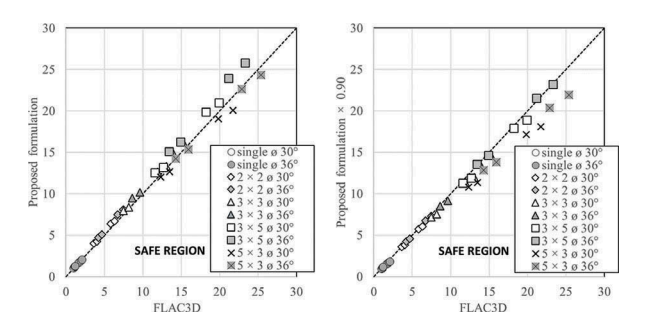


Figure 6. Predicted vs computed pile group capacity [MN]. Left: uncorrected values. Right: reduced values using 0.90 factor in proposed formulation.

5 CONCLUSIONS

Forty FLAC3D numerical analyses of laterally loaded single piles and pile groups in uniform dry sands have been performed. Obtained results have been used as benchmarks to define a simple procedure to calculate ultimate capacity of pile groups with fixed head condition.

Numerical analyses of single piles revealed that established design equations such as Broms (1964a, b) formulation very well agree with numerical results. Moreover, it has been realized that interface friction δ between pile and soil provides a significant contribution to pile capacity. This can be incorporated in the Broms equations by simply using appropriate K_P values.

As for pile groups, a block failure mechanism has been investigated, showing that such assumption well fits numerical results, provided side resistance of such block is related to K_P as well.

A simple procedure and a closed form equation for group efficiency limited to regular pile patterns and to s/D=3 is proposed. It should be emphasized that the proposed procedure is limited to the assessment to ultimate group capacity: in other words, it does not aim at offering a general procedure for elastoplastic analysis of groups including a reliable estimate of group deformation or force distribution among different piles. For general pile group analysis, reference can be made to abundant available literature (e.g. Russo 2016, Ashour et al. (2004), Stacul & Squeglia (2018)) or to available engineering software.

A merit of the proposed procedure, beyond its simplicity, is a clear emphasis to appropriate structural detailing required to ensure the real validity of the proposed design.

Further work is required to investigate the role of additional parameters such as surface surcharge and different pile spacings. An extended comparison with experimental data would also be very valuable, albeit, for the time being, relevant difficulties may be envisaged in the light of practical and economic implications in running realistic lateral loads tests for pile groups.

REFERENCES

Ashour M., Pilling P. and Norris G. 2004. Lateral Behavior of Pile Groups in Layered Soils. J. *Geotech. Geoenviron. Eng.* ASCE, vol. 130: 580–592.

Broms B.B. 1964a. Lateral resistance of piles in cohesionless soils. *ASCE J. Soil Mech. And Found. Div.*, 90(SM3): 123–156.

Broms B.B. 1964b. Lateral resistance of piles in cohesive soils. *ASCE J. Soil Mech. and Found. Div.*, 90 (SM2): 27–63.

Callisto L. & Rampello S. 2013. Capacity Design of Retaining Structures and Bridge Abutments with Deep Foundations. *Journal of Geotechnical and Geoenvironmental Engineering*, ASCE, Vol. 139, No. 7: 1086–1095.

Cecconi M., Pane V., Isidori F. 2006. Un'estensione della Teoria di Broms nel calcolo dei pali sollecitati da forze orizzontali. *V Convegno Nazionale dei Ricercatori in Ingegneria Geotecnica*, Bari (Italy), 15–16 settembre 2006:295–311.

Fayyazi M. S., Taiebat M. and Finn W.D. L. 2014. Group reduction factors for analysis of laterally loaded pile groups. *Can. Geotech. J.* 51: 758–769.

Fleming W. G. K., Weltman A. J., Randolph M. F., Elson W. K. 2009. *Piling Engineering*. 2nd ed., Taylor & Francis, Inc.

Itasca Inc. 2018. FLAC3D. Version 6.0

Lancellotta R. 2007. Lower-bound approach for seismic passive earth resistance. Géotechnique. Vol. 57, No. <pg>3: 319–321.

Patra N. R. and Pise P. J. 2001. Ultimate Lateral Resistance of Pile Groups in Sand. *Journal of Geotechnical and Geoenviromental Engineering*, ASCE, Vol.127, No. 6: 481–487.

Rollins K.M., Lane J.D., Gerber T.M. 2005. Measured and computed lateral response of a pile group in sand. *Journal of Geotechnical and Geoenvironmental Engineering*, ASCE, 131 (1): 103–1114.

Russo G. 2016. A method to compute the non-linear behavior of piles under horizontal loading. *Soils and Foundations*. 56(1): 33–43.

Stacul S. and Squeglia N. 2018. Analysis Method for Laterally Loaded Pile Groups Using an Advanced Modeling of Reinforced Concrete Sections. *Materials*, 11, 300

Viggiani C., Mandolini A., Russo G. 2012. Piles and Pile Foundations. Spon Press.